

## Sensitive gas sensor embedded in a vertical polymer space-charge-limited transistor

Hsiao-Wen Zan, Chang-Hung Li, Chih-Kuan Yu, and Hsin-Fei Meng

Citation: *Applied Physics Letters* **101**, 023303 (2012); doi: 10.1063/1.4734498

View online: <http://dx.doi.org/10.1063/1.4734498>

View Table of Contents: <http://scitation.aip.org/content/aip/journal/apl/101/2?ver=pdfcov>

Published by the [AIP Publishing](#)

---

### Articles you may be interested in

[CSA doped polypyrrole-zinc oxide thin film sensor](#)

*AIP Conf. Proc.* **1512**, 500 (2013); 10.1063/1.4791130

[High output current in vertical polymer space-charge-limited transistor induced by self-assembled monolayer](#)

*Appl. Phys. Lett.* **101**, 093307 (2012); 10.1063/1.4748284

[High-performance space-charge-limited transistors with well-ordered nanoporous aluminum base electrode](#)

*Appl. Phys. Lett.* **99**, 093306 (2011); 10.1063/1.3632045

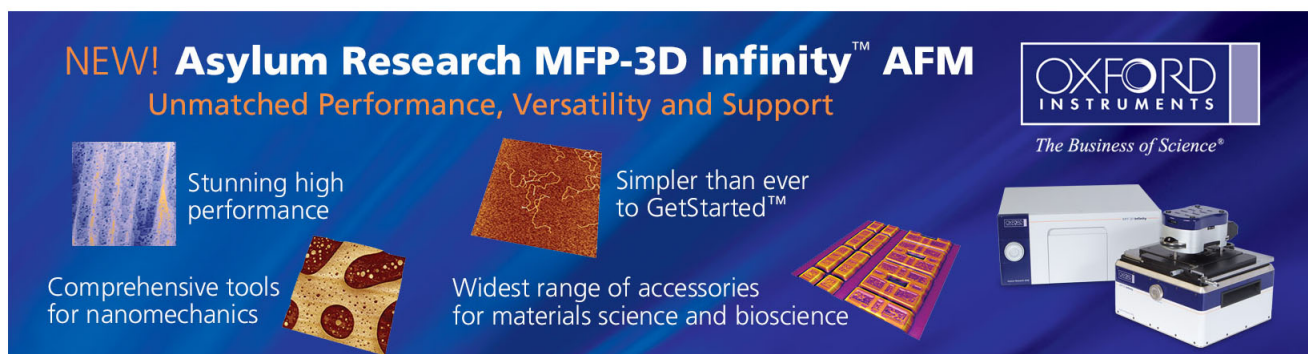
[Polymer space-charge-limited transistor as a solid-state vacuum tube triode](#)

*Appl. Phys. Lett.* **97**, 223307 (2010); 10.1063/1.3513334

[Low voltage active pressure sensor based on polymer space-charge-limited transistor](#)

*Appl. Phys. Lett.* **95**, 253306 (2009); 10.1063/1.3266847

---



**NEW! Asylum Research MFP-3D Infinity™ AFM**  
Unmatched Performance, Versatility and Support

**OXFORD INSTRUMENTS**  
*The Business of Science®*

Stunning high performance  
Simpler than ever to GetStarted™  
Comprehensive tools for nanomechanics  
Widest range of accessories for materials science and bioscience

The advertisement features several images: a blue textured surface, a brown textured surface, a grid of colorful rectangular samples, and the Asylum Research MFP-3D Infinity AFM instrument.

## Sensitive gas sensor embedded in a vertical polymer space-charge-limited transistor

Hsiao-Wen Zan,<sup>1,a)</sup> Chang-Hung Li,<sup>1</sup> Chih-Kuan Yu,<sup>1</sup> and Hsin-Fei Meng<sup>2</sup>

<sup>1</sup>Department of Photonics and Institute of Electro-Optical Engineering, National Chiao Tung University, Taiwan

<sup>2</sup>Institute of Physics, National Chiao Tung University, Taiwan

(Received 23 May 2012; accepted 17 June 2012; published online 11 July 2012)

We report a very sensitive gas sensor embedded in a vertical polymer space-charge-limited transistor. The oxidizing and reducing gases act as electron dedoping and electron doping agents on the transistor active layer to change the potential distribution in the vertical channel and hence to change the output current density. With a 30-ppb detection limit to ammonia, the sensor can be used for non-invasive breath monitor in point-of-care applications. The integration of a sensitive gas sensor and a low-operation-voltage transistor in one single device also facilitates the development of low-cost and low-power-consumption sensor array. © 2012 American Institute of Physics.

[<http://dx.doi.org/10.1063/1.4734498>]

Organic semiconductor materials (OSMs) have been investigated and applied to thin-film transistors because of the low-cost and large-area fabrication on flexible substrates.<sup>1</sup> The gas-sensing ability of OSMs is an unique property that allows the integration of vapor sensors with organic thin-film transistors (OTFTs), which has been extensively studied recently.<sup>2,3</sup> However, high operation voltage ( $>10$  V) is usually required in these OTFT-based gas sensor. Sensitivity may be limited because the gas molecules mostly contact with bulk area (the exposing area) rather than channel area (buried under bulk region).<sup>4,5</sup> In this work, we propose a gas sensor based on a vertical polymer transistor. The current flows in the bulk region of the vertical channel. Exposing the vertical channel to gas molecules creates a significant interaction between channel and gas molecules and hence a high gas sensitivity.

The vertical polymer transistor is called a space-charge-limited transistor (SCLT). In our previous works, we had demonstrated that SCLT exhibits a high on/off current ratio ( $>10\,000$ ) at a low operation voltage ( $<2$  V). The operational mechanism of the vertical polymer SCLT is similar to the solid-state vacuum tube triode.<sup>6</sup> The hole current from the bottom (emitter) to the top (collector) of the bottom-injection SCLT is modulated by the metal-grid, which forms the base terminal of the vertical channel. The bias of the metal-grid controls the potential profile in the vertical channel and hence switches the on and off states of SCLT. It has been demonstrated that SCLT exhibits a very low switching swing, indicating that a slight change of the potential barrier results in a significant current variation when SCLT is biased in the switching transition region.<sup>7</sup> In this work, we demonstrate that the low switching swing of SCLT is critical to provide high gas sensitivity. The lowest detectable ammonia concentration is 30 ppb for a poly(3-hexylthiophene) (P3HT) SCLT. On the other hand, for P3HT OTFT with a conventional bottom-gate structure, the detection limit to ammonia gas is larger than 1 ppm.<sup>2</sup> In literatures, it is known that ammonia molecules ( $\text{NH}_3$ ) act like electron donors to pro-

vide additional electrons to recombine holes in P3HT and hence lower down the conductivity in P3HT.<sup>8–10</sup> In this work, by using computer-aided simulator, we demonstrate that SCLT is sensitive to electron doping in channel region. The simulated response of SCLT to channel electron doping agrees well with the experimental response of SCLT to ammonia molecules. The high sensitivity to ammonia achieved in this work enables the development of non-invasive breath ammonia analysis for monitoring dysfunction of the human body.<sup>11</sup> For such applications, a portable and real-time ammonia sensor with a detection limit of 50 ppb is critical but is still challenging.<sup>11</sup> Our results may facilitate the development of low-cost point-of-care technology.

Three-dimensional and two-dimensional SCLT schematic diagrams are shown in Fig. 1(a); a scanning electron microscope (SEM) image of SCLT is shown in Fig. 1(b). We prepared an indium tin oxide (ITO) glass substrate as the emitter (E). Cross-linkable poly(4-vinyl phenol) (PVP) (8 wt. %) (Mw approximately 20 000, Aldrich) and cross-linking agent poly(melamine-co-formaldehyde) (PMF) were dissolved in propylene glycol monomethyl ether acetate (PGMEA) with a PVP:PMF mass ratio of 11:4. The solution was then spun onto ITO at 1600 rpm for 40 s and annealed at 200 °C for 1 h to form a 200 nm-thick organic dielectric layer. A 1.5 wt. % P3HT (RR  $> 98.5\%$ , Rieke Metals Inc.) solution dissolved in chlorobenzene was then spun onto PVP to form a 20 nm thick layer. The substrate was spin-rinsed with *p*-xylene to increase the P3HT surface polarity. The substrate was then immersed into a solution of 100 nm-diameter negatively charged polystyrene (PS) balls. After the PS balls had adhered to the P3HT surface, 40 nm-thick Al metal was deposited onto the prepared PVP substrate by thermal evaporation, to serve as the base (B). We used Scotch tape (3M) to remove the PS balls and reveal the metal-grid base.  $\text{O}_2$  plasma at 100 W was applied to etch the bare PVP for 8 min, to form vertical channels. A 400 nm-thick P3HT active layer was spun onto the substrate and was annealed at 200 °C for 10 min. The substrate was immersed into a solution of 100 nm-diameter PS balls again. Once the balls had adhered to the P3HT surface, a 40 nm-thick Al

<sup>a)</sup> Author to whom correspondence should be addressed. Electronic mail: [hsiaowen@mail.nctu.edu.tw](mailto:hsiaowen@mail.nctu.edu.tw).

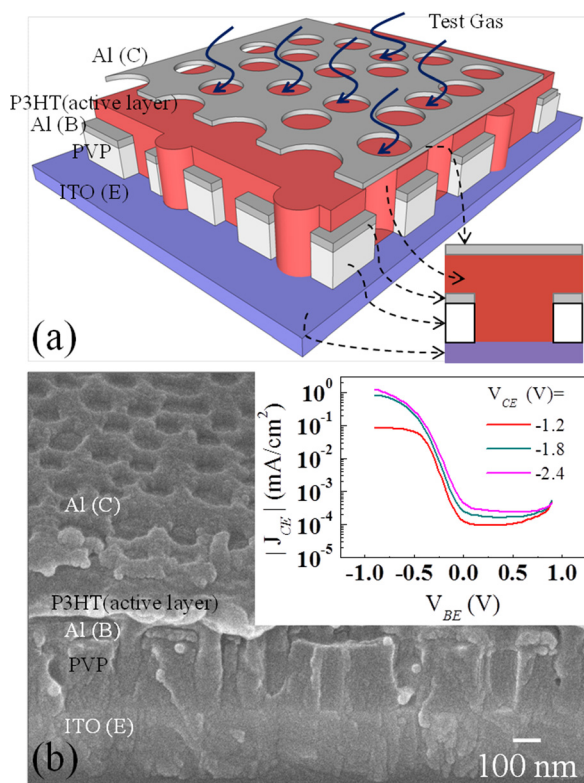


FIG. 1. (a) The three-dimensional and two-dimensional porous SCLT schematic diagrams; (b) The SEM cross-section image of the porous SCLT. Inset of (b) shows the transfer characteristics of the porous SCLT.

layer was deposited by thermal evaporation. The PS balls were then removed by tape to form a collector (C) electrode with high-density nano-meter pores. The test gas easily interacted with the active layer via the nano-meter pores. The transfer characteristics, the collector current density ( $J_{CE}$ ) as a function of the base voltage ( $V_{BE}$ ), of the SCLT with porous collector (porous SCLT) are shown in the inset of Fig. 1(b). With a collector bias ( $V_{CE}$ ) as  $-2.4$  V, porous SCLT exhibits an on/off current ratio as 4750 and a switching swing as 140 mV/dec. When porous SCLT is biased at  $V_{CE} = -1.2$  V, on/off ratio and switching swing are 890 and 122 mV/dec, respectively.

Before analyzing the experimental gas sensing response, we used TCAD SILVACO ATLAS software to simulate the potential distribution in the vertical channel and the ideal transfer characteristics of SCLT. Particularly, to reflect the ammonia sensing response, the influences of electron doping (e-doping) on SCLT are investigated. In literatures, ammonia molecules diffuse into P3HT layer to serve as e-doping agents.<sup>9,10</sup> To discuss equilibrium condition, we assume uniform e-doping distribution in the whole P3HT layer. Material parameters of TCAD simulation were defined in Ref. 12. Figures 2(a) and 2(b) show 2-dimensional potential profiles of the vertical SCLT channel for e-doping concentrations of  $10^{15}$  and  $10^{16}$ , respectively. SCLT is biased in off state with  $V_{CE} = -1.2$  V and  $V_{BE} = 1.5$  V. It is observed that increasing e-doping concentration in P3HT results in the increase of the potential barrier, particularly in the central region of the vertical channel. The potential distributions along the central vertical channel from top Al (C) to bottom ITO (E) with various e-doping concentrations are plotted in Fig. 2(c). As e-doping concentration

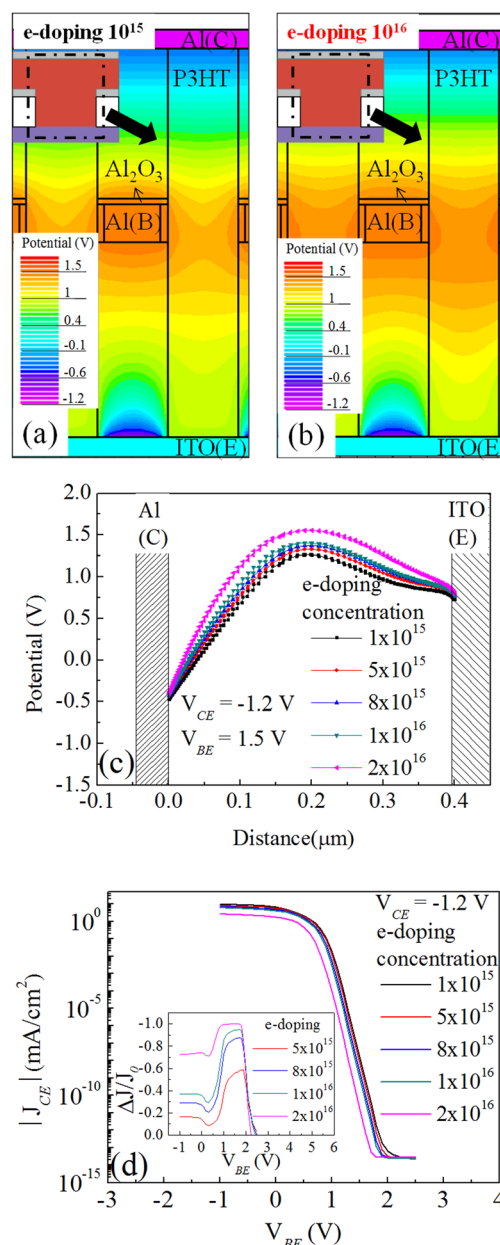


FIG. 2. The two-dimensional potential distribution of P3HT SCLT with e-doping concentration as (a)  $10^{15}$  and (b)  $10^{16}$   $\text{cm}^{-3}$  at  $V_{CE} = -1.2$  V and  $V_{BE} = 1.5$  V. (c) A simulated potential distribution at the central vertical channel from bottom to top. (d) The corresponding simulated  $J_{CE} - V_{BE}$  curves with various e-doping concentrations. Inset of (d) shows the current density variation ratio ( $\Delta J/J_0$ ) as a function of  $V_{BE}$ .

increases, the potential barrier increases. The corresponding ideal  $J_{CE} - V_{BE}$  curves are shown in Fig. 2(d). With a fixed  $V_{CE}$  as  $-1.2$  V,  $J_{CE} - V_{BE}$  curves shifts to the left when e-doping concentration increases, indicating that a more negative base potential is required to lower down the channel potential barrier and to turn on the transistor. To further verify the influence of e-doping on channel potential barrier, the current density variation ratios ( $\Delta J/J_0$ ) as a function of  $V_{BE}$  for various doping concentrations are plotted in the inset of Fig. 2(d). The current density variation ratio ( $\Delta J/J_0$ ), representing the response sensitivity, is defined as  $(J_{CE} - J_{CE0})/J_{CE0}$ , where  $J_{CE0}$  is the collector current density at a electron doping concentration of  $10^{15}$   $\text{cm}^{-3}$ . We found that  $\Delta J/J_0$  is strongly dependent on  $V_{BE}$  and the maximum  $\Delta J/J_0$  is

obtained in the switching region (e.g.,  $0.5\text{ V} < V_{BE} < 2\text{ V}$  in this case). As aforementioned, when SCLT is biased in the switching region, a slight change of base potential causes a significant current variation. The maximum  $\Delta J/J_0$  in the switching region indicates that porous SCLT biased in the switching region exhibits largest response to e-doping as well as the gas molecule interaction. When  $V_{CE}$  is  $-2.4\text{ V}$ , simulated  $\Delta J/J_0$  also has a peak value in the switching region (not shown).

The experimental gas sensing response is then investigated. Two kinds of gas molecules, ammonia and nitric oxide, are used to serve as acceptor (i.e., e-doping) and donor (i.e., hole doping) to P3HT, respectively.<sup>10</sup> The porous SCLT was placed in a micro-fluid sensing chamber containing an atmosphere of high purity (99.9999%) nitrogen gas. We used an electrical syringe pump system to inject the test gas ( $\text{NH}_3$ , 99.9999% pure) into a tube to mix with the  $\text{N}_2$ . The gas mixture then entered the micro-fluid system. The amount of  $\text{N}_2$  was controlled by a mass-flow controller, and specific concentrations of test gas were obtained by adjusting the injection speed of the syringe pump. The concentration of nitric oxide (NO) gas was controlled by a mass-flow controller.

Figure 3(a) shows a plot of  $J_{CE} - V_{BE}$ , representing the porous SCLT's sensing response to  $\text{NH}_3$ .  $V_{CE}$  was fixed as  $-1.2\text{ V}$  and the  $\text{NH}_3$  concentrations were ranged from 30 ppb to 1000 ppb. The response of the switching region

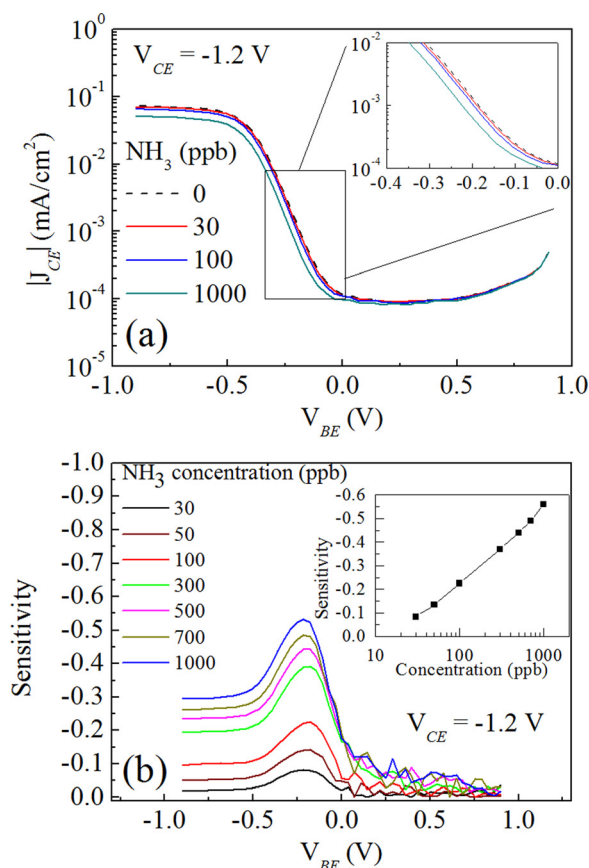


FIG. 3. (a) A plot of  $J_{CE} - V_{BE}$  of porous SCLT under various  $\text{NH}_3$  concentrations. Inset of (a) shows the response to  $\text{NH}_3$  in the switching region ( $V_{BE} = -0.4\text{ V}$  to  $0\text{ V}$ ) of  $J_{CE} - V_{BE}$ . (b) The sensing sensitivities  $\Delta J/J_0$  as a function of  $V_{BE}$  for various  $\text{NH}_3$  concentrations. Inset of (b) shows the maximum sensitivity as a function of  $\text{NH}_3$  concentration.

( $V_{BE} = -0.4\text{ V}$  to  $0\text{ V}$ ) of  $J_{CE} - V_{BE}$  plot is shown in the inset of Fig. 3(a). Increasing  $\text{NH}_3$  concentration makes  $J_{CE} - V_{BE}$  curves shift to the left, indicating an increase of the potential barrier in the vertical channel. This sensing response agrees well with the simulation results for  $J_{CE} - V_{BE}$  described in Fig. 2(d). The sensing sensitivities  $\Delta J/J_0$  as a function of  $V_{BE}$  for various  $\text{NH}_3$  concentrations are plotted in Fig. 3(b). We found that the sensitivity was strongly dependent on  $V_{BE}$ , and that the maximum sensitivity occurred in the switching zone ( $-0.5\text{ V} < V_{BE} < 0\text{ V}$ ). As anticipated, the experimental results agree well with the simulated results in the inset of Fig. 2(d). For  $\text{NH}_3$  concentrations of 30 ppb, 100 ppb, and 1000 ppb, the maximum sensitivities measured at  $V_{BE} = -0.2\text{ V}$  and  $V_{CE} = -1.2\text{ V}$  are  $-0.09$ ,  $-0.23$ , and  $-0.56$ , respectively. As shown in the inset of Fig. 3(b), a power law relationship is found between the maximum sensitivity and  $\text{NH}_3$  concentration, indicating that the proposed  $\text{NH}_3$  sensor is particularly sensitive in low-concentration regime (i.e., 30 ppb to 1000 ppb). Note that when  $V_{CE}$  is  $-2.4\text{ V}$ , the maximum sensitivity to 100-ppb  $\text{NH}_3$  is  $-0.19$  at  $V_{BE} = -0.2\text{ V}$ . Compared to porous SCLT biased at  $V_{CE} = -1.2\text{ V}$ , porous SCLT biased at  $V_{CE} = -2.4\text{ V}$  exhibits a larger initial on/off current ratio as 4750 but a slightly degraded  $\text{NH}_3$  sensitivity. The large on/off ratio is due to the large on current. Since the sensing response is defined as the current variation ratio, the large on current also serves as a large background signal to suppress the  $\text{NH}_3$  sensing response.

Since the proposed sensor is embedded in a vertical transistor, it is therefore important to evaluate the switching properties of the transistor under  $\text{NH}_3$  sensing. The switching function of the porous SCLT under  $\text{NH}_3$  sensing is shown in Fig. 4(a). The porous SCLT is biased at  $V_{CE} = -1.7\text{ V}$  to exhibit an initial on/off current ratio as 3300 and a good

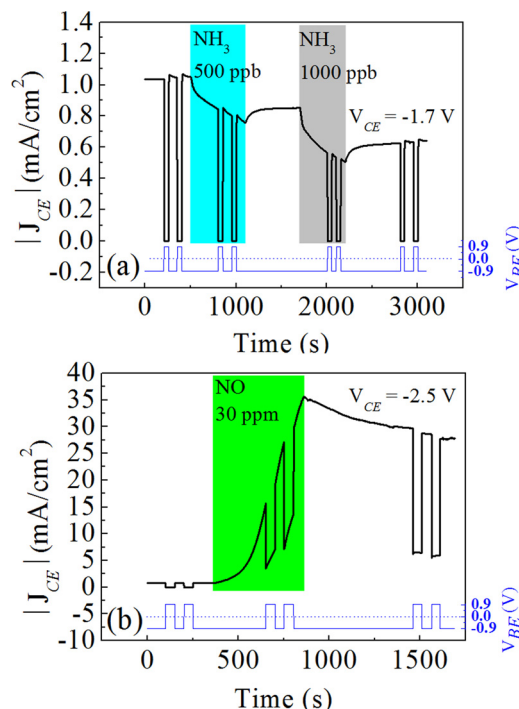


FIG. 4. The real-time sensing switching function of porous SCLT under (a)  $\text{NH}_3$  and (b) NO.

enough sensitivity to  $\text{NH}_3$ . The porous SCLT exhibits a significant current drop under  $\text{NH}_3$  sensing (the shaded areas). During  $\text{NH}_3$  sensing, a good on/off switching property is still obtained when switching  $V_{BE}$  between  $-0.9$  V (on state) and  $0.9$  V (off state). This result suggests that the proposed porous SCLT integrates a  $\text{NH}_3$  sensor and a switching transistor in one single device. In sensor array technology, to save the operational power and to improve the signal-to-noise ratio, the pixel circuit is composed of one sensor and one switching transistor.<sup>13</sup> Our proposed device can serve as a pixel circuitry by itself, facilitating the development of low-power sensor array technology. After removing  $\text{NH}_3$ , the recovery behavior is found to be dependent on  $V_{BE}$  (not shown). A  $-0.9$ -V  $V_{BE}$  bias (on state) causes a poor recovery while a  $0$ -V or  $+0.9$ -V  $V_{BE}$  bias (off state) for  $600$  s leads to an almost complete recovery of the current level. The negative  $V_{BE}$  bias may attract  $\text{NH}_4^+$  ions, which are generated by the decomposition of  $\text{NH}_3$ , and hence impede the desorption of  $\text{NH}_3$ .<sup>14</sup>

In addition to study the sensor response to e-doping agents like  $\text{NH}_3$ , the response to hole doping agents is also investigated. Fig. 4(b) shows the real-time sensing response of  $J_{CE}$  to NO. To observe the influences of NO on both on and off state of the transistor, porous SCLT is biased at  $V_{CE} = -2.5$  V to exhibit a large initial on/off current ratio as  $5000$ . In opposite to the current-drop response to  $\text{NH}_3$ , the sensor exhibits a significant current increase when NO is injected into the sensing chamber. Since NO is known to serve as the hole doping agents on P3HT,<sup>15</sup> it is suggested that hole concentrations in P3HT is increased and the hole current is also increases during NO sensing. The increased hole concentration in P3HT, however, deteriorates the switching function of SCLT. As shown in the shaded area (NO sensing area), off-state current increases significantly when SCLT is biased at  $V_{BE} = 0.9$  V (off state). The poor base control over the channel potential may be due to the base-field shielding effect (or the screening effect) when P3HT is doped by hole-doping agents. Similar base-field shielding effects in SCLT have been observed in our previous reports when we added the tetrafluoro-tetracyano-quinodimethane (F4-TCNQ) to dope P3HT or when we irradiated light to create electron-hole pairs in P3HT.<sup>16,17</sup> A poor recovery is also found in NO sensing as shown in Fig. 4(b). Changing  $V_{BE}$  no longer improves the recovery. The poor recovery when exposing conducting polymers to strong oxidizing gases was also observed in other reports.<sup>18</sup> The mechanism is still not clear.

In summary, we proposed a low-power sensitive gas sensor embedded in a vertical polymer transistor, SCLT. In

SCLT, current flows in the bulk region of the vertical channel. Exposing the vertical channel to gas molecules creates a significant interaction between channel and gas molecules and hence a high gas sensitivity. Moreover, the potential profile in the vertical channel is sensitive to the channel doping concentration as well as the base bias. When P3HT-based porous SCLT is biased in the switching region, a maximum sensitivity to  $\text{NH}_3$  can be obtained with a detection limit as  $30$  ppb. The sensitivity is much higher than P3HT-based OTFT, which has a  $\text{NH}_3$  detection limit higher than  $1$  ppm. The high  $\text{NH}_3$  sensitivity achieved in this work facilitates the development of non-invasive breath ammonia analysis for point-of-care applications. The proposed sensor integrating a gas sensor and a switching transistor in one single device also can be used as pixel circuitry in sensor array applications.

This work was supported in part by the National Science Council under Grant 100-2628-E-009-018-MY3 and 100-2628-M-009-002.

<sup>1</sup>B. Crone, A. Dodabalapur, Y. Y. Lin, R. W. Filas, Z. Bao, A. LaDuca, R. Sarapeshkar, H. E. Katz, and W. Li, *Nature (London)* **403**, 521 (2000).

<sup>2</sup>J. W. Jeonga, Y. D. Leea, Y. M. Kima, Y. W. Parka, J. H. Choia, T. H. Parka, C. D. Soob, S. M. Wonb, I. K. Hanc, and B. K. Jua, *Sens. Actuator B* **146**, 40 (2010).

<sup>3</sup>R. S. Dudhe, S. P. Tiwari, H. N. Raval, M. A. Khaderbad, R. Singh, J. Sinha, M. Yedukondalu, M. Ravikanth, A. Kumar, and V. R. Rao, *Appl. Phys. Lett.* **93**, 263306 (2008).

<sup>4</sup>B. Li and D. N. Lambeth, *Nano Lett.* **8**, 3563 (2008).

<sup>5</sup>A. N. Sokolov, M. E. Roberts, and Z. Bao, *Mater. Today* **12**, 12 (2009).

<sup>6</sup>Y. C. Chao, M. C. Ku, W. W. Tsai, H. W. Zan, H. F. Meng, H. K. Tsai, and S. Fu Horng, *Appl. Phys. Lett.* **97**, 223307 (2010).

<sup>7</sup>Y. C. Chao, H. K. Tsai, H. W. Zan, Y. H. Hsu, H. F. Meng, and S. F. Horn, *Appl. Phys. Lett.* **98**, 223303 (2010).

<sup>8</sup>G. Bischoff and W. F. Schmidt, *Macromol. Mater. Eng.* **208**, 151 (1993).

<sup>9</sup>F. Mohammad, *J. Phys. D: Appl. Phys.* **31**, 951 (1998).

<sup>10</sup>H. Bai and G. Shi, *Sensors* **7**, 267 (2007).

<sup>11</sup>T. Hibbard and A. J. Killard, *Crit. Rev. Anal. Chem.* **41**, 21 (2011).

<sup>12</sup>The SCLT characteristics simulation is made based on the device structure shown in Fig. 2. The thicknesses of PVP, Al grid,  $\text{Al}_2\text{O}_3$ , and P3HT are  $200$ ,  $40$ ,  $10$ , and  $400$  nm, respectively. The opening diameter is  $100$  nm. The highest occupied molecular orbital and lowest unoccupied molecular orbital levels of P3HT are  $5.2$  and  $3.0$  eV. The work functions of emitter and collector are  $5.2$  and  $4.3$  eV. The hole mobility and electron mobility in P3HT are  $10^{-5}$  and  $10^{-6}$   $\text{cm}^2/\text{V s}$ .

<sup>13</sup>B. Guo, A. Bermak, P. C. H. Chan, and G. Z. Yan, *Solid-State Electron.* **51**, 69 (2007).

<sup>14</sup>P. Foot, T. Ritchie, and F. Mohammad, *J. Chem. Soc., Chem. Commun.* 1536–1537 (1988).

<sup>15</sup>V. Saxena, D. K. Aswal, M. Kaur, S. P. Koiry, S. K. Gupta, J. V. Yakhmi, R. J. Kshirsagar, and S. K. Deshpande, *Appl. Phys. Lett.* **90**, 043516 (2007).

<sup>16</sup>Y. C. Chao, C. Y. Chen, H. W. Zan, and H. F. Meng, *J. Phys. D: Appl. Phys.* **43**, 205101 (2010).

<sup>17</sup>H. W. Zan, W. W. Tsai, and H. F. Meng, *Appl. Phys. Lett.* **98**, 053305 (2011).

<sup>18</sup>M. K. Ram, O. Yavuz, and M. Aldissi, *Synth. Met.* **151**, 77 (2005).